Dynamic positive column in long-gap barrier discharges

A. Shvydky,[a] V. N. Khudik, and C. E. Theodosiou
Department of Physics and Astronomy, University of Toledo, Toledo, Ohio 43606

V. P. Nagorny
Plasma Dynamics Corporation, Waterville, Ohio 43566

(Received 7 March 2005; accepted 18 November 2005; published online 9 January 2006)

A simple analytical model of the barrier discharge in a long gap between opposing plane electrodes is developed. It is shown that the plasma density becomes uniform over a large part of the gap in the course of the discharge development, virtually forming a dynamic positive column. The column completely controls the dynamics of the barrier discharge and determines such characteristics as the discharge current, discharge duration, light output, etc. Using the proposed model, one can easily evaluate many important discharge parameters. © *2006 American Institute of Physics*.
[DOI: 10.1063/1.2158139]

I. INTRODUCTION

Dielectric barrier discharges are typically generated in gas gaps between two electrodes covered with dielectric layers by applying to the electrodes a sinusoidal or square-wave voltage with frequencies in the range from a few kilohertz to hundreds of kilohertz. The product of the gas pressure and the distance between the dielectric surfaces (pD) in these discharges can vary quite significantly. In the present paper we consider barrier microdischarges such as those used in plasma display panels (PDP's),[1] where $pD \sim 5-50$ Torr $\times$ cm.

The one-dimensional (1D) barrier discharge was studied in a number of works[2–5] where detailed PDP models were developed. Computer simulations performed using these models are capable of accurate reproduction of many features of the PDP discharges. They help to uncover general trends in the discharge behavior and thus to build analytical theories.

An analytical theory of the dynamics of a 1D barrier discharge during one pulse of the applied square-wave voltage was developed in our previous work.[6] It was shown that at high overvoltage the discharge develops into an ionization wave whose velocity is determined primarily by the charge production rate in the cathode fall region. This wave moves from the anode toward the cathode, resulting in a contraction of the cathode fall region and an increase of the electric field within this region. Upon reaching the cathode, the ionization wave can either quickly disappear (when the capacitance of the dielectric layer is small) or transform into a quasistationary dc cathode fall (when the capacitance is large). The main assumption of this previous work[6] was that the resistance of the plasma trail, created by the ionization wave, can be neglected.

In the present paper we consider the opposite case, when the barrier discharge dynamics is strongly influenced by the plasma trail. As will be shown below, in the case of long-gap barrier discharges, the plasma trail becomes uniform over a large part of the gap, virtually forming a dynamic positive column—the column whose density changes with time. Similar to dc discharges, the positive column in barrier discharges is a quite efficient source of light (radiation),[7] and therefore the study of properties of the dynamic positive column is important for PDP applications.

The uniformity of the column enables us to consider it simply as a variable resistor through which the cathode fall (CF) charges the dielectric layer capacitor. When this capacitance is large, one can introduce further simplifications into the model. In this case during the large-current stage of the discharge development, the CF is, in essence, quasistationary and its V-I characteristics can be approximated by those of the dc cathode fall.[8]

The plan of the paper is as follows. Based on computer simulations (similar to Ref. 5), we give in Sec. II a qualitative consideration of long-gap large-capacitor discharges and then derive the basic equations of our analytical model. Although this model does not have a rigorous mathematical foundation based on the first principles of the discharge theory, it agrees quite well with the simulations over a wide range of discharge parameters. In Sec. III, we solve analytically the basic equations of the model in the case when the voltage across the CF can be considered constant during the large-current stage of the discharge development. Predictions of the model are discussed in Sec. IV.

II. QUALITATIVE CONSIDERATION AND BASIC EQUATIONS

We will study the dynamics of a 1D barrier discharge during one pulse of an applied square-wave voltage in a gas-filled gap between opposing plane electrodes covered by dielectric layers of thickness d and dielectric constant ϵ (see Fig. 1). It is assumed that the dielectric layer capacitance is large, i.e., the effective thickness of the dielectric layers is small,

$$2d/\epsilon \lesssim L_{\mathrm{norm}}, \tag{1}$$

where L_{norm} is the normal CF length.[8] The gap length L_g is taken to be much larger than the length L_{norm},

[a]Electronic mail: ashvidk@physics.utoledo.edu

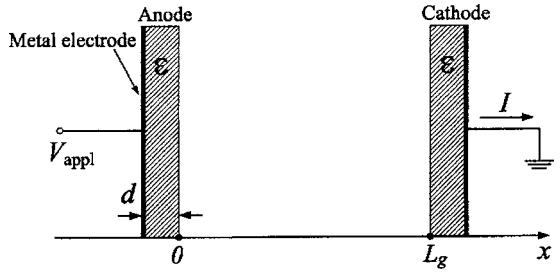

FIG. 1. Basic geometry of the discharge.

$$L_g \gg L_{\text{norm}}. \tag{2}$$

This inequality is always satisfied under typical discharge conditions in a PDP cell. For example, in the case 10% Xe/90% Ne mixture at a pressure $p=500$ Torr and with secondary electron emission coefficients $\gamma_{\text{Ne}}=0.5$ and $\gamma_{\text{Xe}}=0.005$, the normal CF length $L_{\text{norm}}\sim 6.5$ μm, while the gap length under consideration is from several hundred microns to 1 mm.

The analysis of extensive computer simulations, performed in the framework of the fluid model,[5] shows that the discharge goes through the following four stages when the discharge gap is long, the dielectric layer capacitor is large, and the applied voltage V_{appl} is sufficiently higher than the breakdown voltage.

(1) *Linear stage*. At the beginning of the discharge, the small discharge current grows at a steady rate and the positive charge accumulates in the gap. The charge created during this stage is small and the distribution of the electric field is almost the same as in the empty gap.

(2) *Breakdown stage*. At some moment, the volume charge reaches a critical value ($\sim\epsilon_0 V_{\text{appl}}/L_g$) and causes considerable distortion of the electric field in the anode region. The field vanishes at the anode, and from this moment on there coexist two different regions in the gap: the region filled with plasma (plasma trail) where the electric field is relatively small and the region of the gap adjacent to the cathode where the electric field is strong and the electron density is negligible. With time, the CF region contracts and the discharge current continues to grow (although it still remains quite small). The electric field increases in the plasma trail, and the trail uniformization begins. During this stage the voltage across the CF region decreases, the voltage across the plasma trail increases, and the voltage on the dielectric layer capacitor is still negligibly small.

(3) *Power deposition stage (large-current stage)*. When the length of the CF region becomes comparable to L_{norm}, the dynamic CF transforms into a quasistationary one (since L_{norm} is larger than $2d/\epsilon$, see Ref. 6). At this moment, the discharge current sharply increases. After some time it reaches its maximum and then decreases. The plasma density in the already uniformized plasma trail monotonically grows and, in contrast to the second stage, the electric field there (as well as the voltage) now falls. Figure 2, where we present the results of fluid simulations, illustrates the dynamics of these processes.

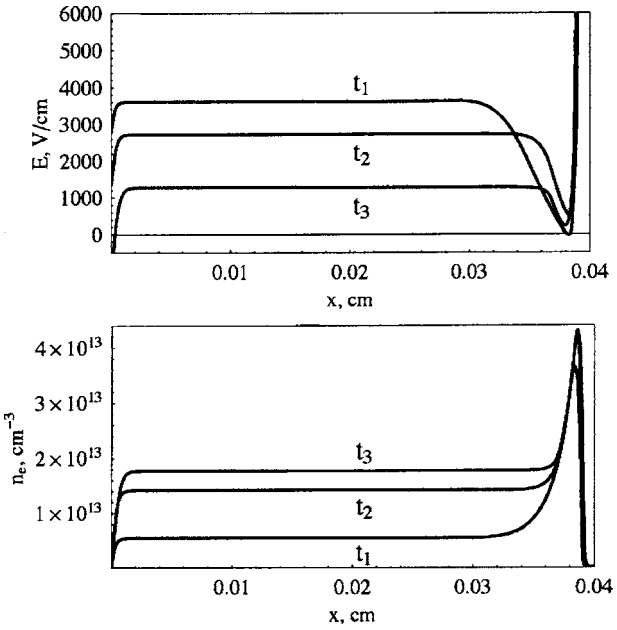

FIG. 2. Electric field E and electron density n_e in the gap at time moments $t_1<t_2<t_3$ when the discharge current is strong: $I(t_1)=0.5I_{\text{max}}$, $I(t_2)=I_{\text{max}}$, and $I(t_3)=0.5I_{\text{max}}$, where I_{max} is the maximum discharge current; $V_{\text{appl}}=300$ V, $L_g=400$ μm, and $2d/\epsilon=1$ μm.

As the strong current charges the dielectric layer capacitor, the voltage on it grows, so that at the end of this stage the main portion of the external voltage drops across this capacitor. The decrease of the voltage across the gas gap leads to quenching of the discharge.

This stage is of great interest because there occurs an intensive deposition of power from the external source into the discharge. Let us note that this stage lasts quite a short time (usually several tens of nanoseconds), and therefore it is not influenced by the relatively slow chemical kinetics of excited species and molecular ions (see, for example, Refs. 5 and 9).

(4) *Afterglow stage*. In the afterglow, which lasts several microseconds, the number of ions and electrons in the gap gradually decreases through the dissociative recombination of electrons and molecular ions. Charged particles are also pulled out of the plasma toward the dielectric surfaces by the residual and ambipolar electric fields. During this stage, the discharge current and the power deposition are small.

The transformation of the dynamic CF into the quasistationary one, which occurs under condition (1) at the beginning of the third stage, can be qualitatively explained in the following way: When the capacitance of the dielectric layers is large compared to the "capacitance" of the CF (i.e., to the ratio of the total charge in the CF to the voltage across the CF), the deposition of the total charge in the CF onto the dielectric does not significantly change the voltage across the dielectric layer capacitor. On the contrary, many generations of ions will have to replace each other in the CF before the voltage across this capacitor noticeably changes.

A remarkable feature of long-gap barrier discharges is that during the third stage, the plasma trail is uniform and

can be treated as a dynamic positive column. Let us qualitatively explain the intrinsic mechanism responsible for the uniformization. Due to the plasma quasineutrality, which is quickly established in the Maxwellian relaxation time (see Ref. 8 and the Appendix), the particle current is constant throughout the plasma trail. Since the conductivity of the plasma is proportional to its density, the electric field E is higher in regions where the plasma density n is lower. The higher electric field results in higher ionization rate, which in turn leads to faster growth of the plasma in these regions and, eventually, to a leveling off of the plasma density. This reasoning can be backed by the following consideration, in which we show that small perturbations of the plasma in the positive column decay.

The discharge current in the plasma trail can be represented as a sum of the electron and ion currents and the displacement current,

$$I(t) = en_e\mu_e SE + en_i\mu_i SE + \epsilon_0 S\frac{\partial E}{\partial t}, \tag{3}$$

where e is the elementary charge, n_e and n_i are the electron and ion densities, μ_e and μ_i are the electron and ion mobilities, and S is the cross-sectional area of the discharge. For simplicity, we neglect in (3) the diffusion components in particle currents. Since the plasma in the trail is quasineutral, $n_e \approx n_i \approx n$, the displacement current is negligibly small compared to the particle current (see Appendix). Also omitting the ion current ($\mu_i \ll \mu_e$), we conclude that

$$I(t) \approx en\mu_e SE. \tag{4}$$

Representing

$$n = n_{\mathrm{pc}} + \delta n, \quad E = E_{\mathrm{pc}} + \delta E, \tag{5}$$

where δn and δE are small spatial perturbations and n_{pc} and E_{pc} are the spatial average values of the plasma density and electric field in the plasma column, we derive from Eq. (4) the simple relationship

$$\delta n E_{\mathrm{pc}} + n_{\mathrm{pc}}\delta E = 0. \tag{6}$$

From the continuity equation for electrons

$$\frac{\partial n}{\partial t} - \frac{\partial n\mu_e E}{\partial x} = r(E)n, \tag{7}$$

where $r(E)$ is the ionization rate, and from Eqs. (4) and (6), one can readily obtain the equations for n_{pc} and δn:

$$\frac{\partial n_{\mathrm{pc}}}{\partial t} = r(E_{\mathrm{pc}})n_{\mathrm{pc}}, \tag{8}$$

$$\frac{\partial \delta n}{\partial t} = \left[r(E_{\mathrm{pc}}) - E_{\mathrm{pc}}\frac{dr(E_{\mathrm{pc}})}{dE_{\mathrm{pc}}} \right]\delta n. \tag{9}$$

While the obvious equation (8) describes the growth of the plasma density in the positive column and the increase of its conductivity $\sigma \approx e\mu_e n_{\mathrm{pc}}$, Eq. (9) shows fast decay of the density perturbations [since under positive column conditions $E_{\mathrm{pc}}r'(E_{\mathrm{pc}}) > r(E_{\mathrm{pc}})$, the prime here denotes the derivative]. Let us emphasize that, as seen from our derivation, the mechanism of the positive column uniformization has an entirely dynamic nature and manifests itself regardless of the diffusion processes [keeping the particle diffusion in Eqs. (3)–(7) leads to the appearance of a convective term in Eq. (9) for the density perturbation and does not affect its decay]. It is interesting to note that the uniformization takes place even in a more general case[10] when the discharge cannot be treated as quasi-one-dimensional.

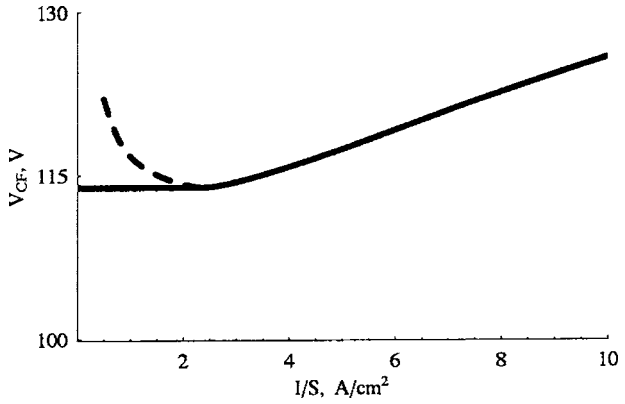

FIG. 3. *V-I* characteristics of the dc cathode fall obtained from fluid simulations for 10% Xe/90% Ne mixture; P=500 Torr, γ_{Ne}=0.5, and γ_{Xe}=0.005. Dashed curve corresponds to the unstable, subnormal cathode fall.

Below we give a simple analytic description of only the third stage of the discharge development (when the discharge current is strong, the positive column is uniform, and the CF is quasistationary). During this stage, the positive column occupies almost the entire gap, so that its resistance is $R \approx L_g/(\sigma S) \approx L_g/(en_{\mathrm{pc}}\mu_e S)$. As seen from this definition and from Eq. (8), the positive column resistance is governed by the equation

$$\frac{dR}{dt} = -r(E_{\mathrm{pc}})R, \tag{10}$$

where

$$E_{\mathrm{pc}} = \frac{V_{\mathrm{pc}}}{L_g}. \tag{11}$$

V_{pc} is the voltage drop across the positive column.

The quasistationarity of the cathode fall allows us to use the *V-I* characteristic of the corresponding dc cathode fall,

$$V_{\mathrm{CF}} = V_{\mathrm{CF}}(I). \tag{12}$$

We took this characteristic from the fluid simulations (see Fig. 3) although, in principle, it can be taken even from experimental data. Adding up the voltages across the elements of the circuit in Fig. 4, one can write the equation

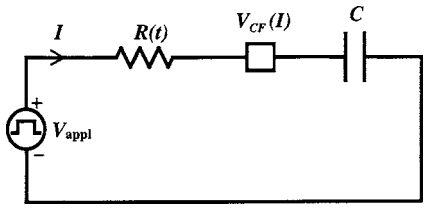

FIG. 4. Equivalent circuit of a long-gap barrier discharge after uniformization of the positive column and formation of a quasistationary CF.

$$V_{pc} + V_{CF}(I) + \frac{q}{C} = V_{appl}, \tag{13}$$

where

$$V_{pc} = IR. \tag{14}$$

$C = \epsilon_0 \epsilon S/2d$ is the capacitance of the dielectric layer capacitor (see Fig. 1), and the capacitor charge q changes with time as

$$\frac{dq}{dt} = I. \tag{15}$$

Equations (10)–(15) form the foundation of our model of barrier discharges with long positive columns and a quasistationary cathode fall; they are solved with the initial conditions

$$R(t \to -\infty) = \infty, \tag{16}$$

$$q(t \to -\infty) = 0. \tag{17}$$

Condition (16) means that the resistance of the positive column at the beginning of the strong-current stage is so high compared to the resistance during the main part of this stage that it can be set to infinity; condition (17) means that the voltage q/C across the capacitance at the beginning of the strong-current stage is negligibly small compared to V_{CF} and V_{appl}.

Our analysis shows that results obtained from our simple model, described by Eqs. (10)–(17), agrees quite well with those obtained from the fluid simulations (under the same discharge conditions) over a very large range of the discharge parameters. It turns out that when the discharge current is not very high and therefore the voltage across the dc cathode fall changes insignificantly (see Fig. 3), the model can be simplified even further by considering V_{CF} to be constant and equal to V_{norm}. In this case, the main characteristics of the barrier discharge are determined by the interplay between the positive column and the capacitor.

III. CONSTANT CF VOLTAGE APPROXIMATION

When $V_{CF} = V_{norm} = \text{const}$, it is convenient to use R and E_{pc} as independent variables. Replacing V_{pc} in Eq. (13) with $E_{pc}L_g$, and then taking the time derivative of this equation and using Eqs. (14) and (15), one can obtain the equation for the electric field in the positive column,

$$\frac{dE}{dt} = -\frac{E}{RC}, \tag{18}$$

where the subscript "pc" is omitted for brevity. The initial condition for this equation directly follows from (17) and Kirchhoff's law (13):

$$E(t \to -\infty) = E_0 \equiv \frac{V_{appl} - V_{CF}}{L_g}. \tag{19}$$

Dividing the left and right parts of Eq. (10) by the corresponding parts of Eq. (18) and multiplying both parts by C, we obtain

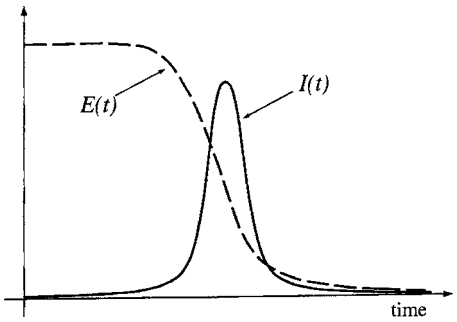

FIG. 5. Typical dependence of I and E on time.

$$\frac{d(RC)}{dE} = \frac{r(E)}{E}(RC)^2. \tag{20}$$

Integrating this equation with the initial conditions (16) and (19) gives

$$\frac{1}{RC} = \bar{r}(E, E_0), \tag{21}$$

where

$$\bar{r}(E, E_0) \equiv \int_E^{E_0} \frac{r(E)}{E} dE. \tag{22}$$

Substitution of (18) and (21) leads to a differential equation for the electric field,

$$\frac{dE}{dt} = -E\, \bar{r}(E, E_0). \tag{23}$$

From this equation, one can see that the time evolution of the electric field in the positive column depends only on its initial value and the ionization rate and does not depend explicitly on the electron mobility. Because the right part of Eq. (23) is always negative, the electric field monotonically decreases with time from E_0 to zero. On the other hand, the discharge current

$$I \equiv \frac{EL_9}{R} = L_g CE\, \bar{r}(E, E_0) \tag{24}$$

goes from zero (at $E = E_0$), through a maximum (at some point $E = E_*$), to zero again (at $E = 0$) (see Fig. 5). The electric field E_* at the current maximum can be found from the condition $dI(E)/dE = 0$, in which the current is taken from Eq. (24). A straightforward calculation gives

$$r(E_*) = \bar{r}(E_*, E_0). \tag{25}$$

The typical shape of the function $r(E)/E$ [which is proportional to the ionization coefficient $\alpha(E)$] as well as the graphical solution of Eq. (25) is given in Fig. 6. From this figure, one can see in particular that $E_0/2 < E_* < E_0$ always If $r(E)/E$ grows faster than a linear function, then $E_0/\sqrt{3} < E_* < E_0$.

Using Eqs. (24) and (25), the expression for maximum current can be written as

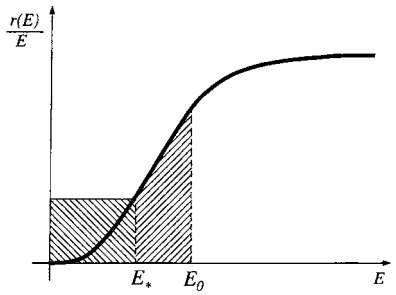

FIG. 6. Graphical solution of Eq. (25). The area of the dashed rectangle on the left is equal to $r(E_*)$, while the area of the dashed region under the $r(E)/E$ curve on the right is equal to $\bar{r}(E_*,E_0)$. These areas are equal when E_* is the electric field at the maximum current.

$$I_{\max} = CL_g E_* r(E_*). \tag{26}$$

This equation shows that in the present model the maximum current is proportional to the dielectric layer capacitance. The dependence on the gap length L_g is more complicated, since E_* also depends on L_g (through E_0).

The time duration τ_{cur} of the current pulse can be defined as the ratio of the transferred charge $Q_{\text{tr}}=C(V_{\text{appl}}-V_{\text{CF}})=CL_gE_0$ to the maximum current,

$$\tau_{\text{cur}} \equiv \frac{Q_{\text{tr}}}{I_{\max}} = \frac{E_0}{E_* r(E_*)}. \tag{27}$$

It is useful to note that when $r(E)/E$ grows faster than linearly, then

$$\tau_{\text{cur}} > \frac{3\sqrt{3}}{r(E_0)} \approx \frac{5.2}{r(E_0)}. \tag{28}$$

For a steeper dependence of the ionization coefficient on the electric field, the numerical coefficient in Eq. (28) is even greater.

Many important characteristics of long-gap discharges can be easily evaluated from the formulas obtained above. For example, from (21) immediately follow the expressions for the resistance of the positive column at the end of the strong current stage,

$$R_f = \frac{1}{C\,\bar{r}(0,E_0)}, \tag{29}$$

and for the plasma density in the column at the end of this stage,

$$n_f = \frac{C\,L_g}{e\mu_e S}\bar{r}(0,E_0). \tag{30}$$

Using the expression for the ionization coefficient $\alpha = r/\mu_e E$ and Eqs. (22) and (30), the ratio of the total number of electrons (ions) created in the positive column $N=n_f L_g S$ to the number of transferred electrons (ions) Q_{tr}/e can be written in the form

$$\frac{eN}{Q_{\text{tr}}} = \langle\alpha\rangle L_g, \tag{31}$$

where

$$\langle\alpha\rangle = \frac{1}{E_0}\int_0^{E_0} \alpha(E)dE.$$

Note that $\langle\alpha\rangle < 0.5\alpha(E_0)$ if $\alpha(E)$ grows faster than linearly. Therefore, there is a practically useful estimate for the number of charged particles created in the positive column,

$$eN \lesssim \tfrac{1}{2}\alpha(E_0)L_g Q_{\text{tr}}. \tag{32}$$

Interestingly, this expression gives reasonable estimates far beyond the applicability of our model. Note that since the electric field is small in the positive column, in the case of noble gas mixtures, mainly the ions of species with the lower ionization potential are created there.

Similar formulas can be obtained for the number of excited atoms (molecules) created in the positive column during the discharge,

$$\frac{eN_{\text{exc}}}{Q_{\text{tr}}} = \langle\alpha_{\text{exc}}\rangle L_g,$$
$$\langle\alpha_{\text{exc}}\rangle = \frac{1}{E_0}\int_0^{E_0} \frac{r_{\text{exc}}(E)}{\mu_e E}dE, \tag{33}$$

where τ_{exc} is the excitation rate. Again, in the case of noble gas mixtures, mostly the species with lower excitation energies get excited.

It follows from Eqs. (23) and (24) that $I=-L_gCdE/dt$. Using this expression and Eq. (19), the energy deposited into the positive column can be estimated as

$$W_{\text{pc}} = \int IEL_g dt = \frac{1}{2}C(V_{\text{appl}}-V_{\text{CF}})^2, \tag{34}$$

while the total energy which goes from the external source into the discharge is

$$W_{\text{tot}} = \tfrac{1}{2}CV_{\text{appl}}^2. \tag{35}$$

Note that the same amount of energy, $CV_{\text{appl}}^2/2$, is stored in the capacitor (it would be recovered during the next discharge pulse in the sustain regime).

The difference between Eqs. (34) and (35) gives the amount of energy that goes into the CF,

$$W_{\text{CF}} = \tfrac{1}{2}C[V_{\text{appl}}^2 - (V_{\text{appl}}-V_{\text{CF}})^2]. \tag{36}$$

IV. DISCUSSION

Let us again point out that the approximation $V_{\text{CF}}=V_{\text{norm}}$ is valid only when the discharge current is not very high. It means that substitution of $I_{\max}$ from Eq. (26) into the *V-I* characteristics of the dc cathode fall (12) must lead to the approximate equality

$$V_{\text{CF}}(I_{\max}) \approx V_{\text{norm}}. \tag{37}$$

If the obtained CF voltage is noticeably higher than the normal CF voltage, one should analyze the full system of Eqs. (10)–(15), i.e., use the more accurate $V_{\text{CF}}=V_{\text{CF}}(I)$ approximation instead of the $V=V_{\text{norm}}$ approximation.

In Figs. 7–9 we compare the results obtained from our model and from fluid simulations under several different dis-

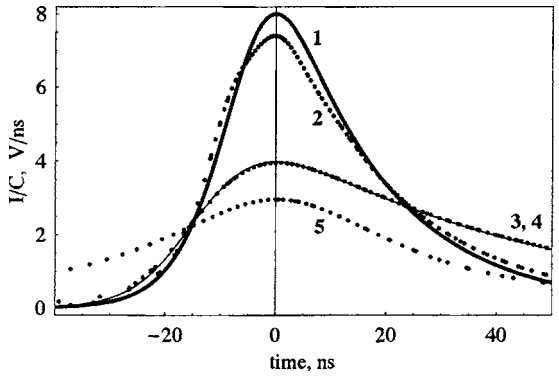

FIG. 7. Renormalized discharge current for $L_g=800$ μm and $V_{\text{appl}}=390$ V: (1) $V_{\text{CF}}=V_{\text{norm}}$ approximation and (2) fluid simulation for $2d/\epsilon=1$ μm, (3) $V_{\text{CF}}=V_{\text{CF}}(I)$ approximation and (4) fluid simulation for $2d/\epsilon=0.1$ μm, and (5) fluid simulation for $2d/\epsilon=10$ μm. Time is measured from the moment of maximum of the currents.

charge conditions. A striking feature of all these figures is that the amplitude of the renormalized current I/C changes by only a factor of 2–3 when the capacitance C changes by two orders of magnitude (compare curves 2, 3, and 5). The prediction of our model that I/C does not depend on C [see Eq. (26)] is qualitatively correct even when criterion (1) of the model applicability is not satisfied. For example, for curve 5, the effective dielectric thickness $2d/\epsilon=10$ μm is greater than the normal CF length $L_{\text{norm}}\approx 6.5$ μm, so that the CF cannot be considered as a quasistationary one!

Understandably, the $V_{\text{CF}}=V_{\text{norm}}$ approximation overestimates the amplitude of the discharge current, since V_{norm} is the minimal voltage on the CF during the large-current stage of the discharge development; this overestimation is more pronounced for shorter gaps.

Another interesting feature of the long-gap-discharge dynamics is that the duration of the current pulse increases with the increase of the gap length (compare Fig. 9 with Figs. 7 and 8), which is not at all obvious since the applied voltage is greater in the case of the longer gap. Qualitatively, this discharge property is attributed to the increase in the inertia of the positive column with the increase of its length.

Note also that in the case of the large capacitance (abnormal quasistationary CF, see curve 3 in Figs. 7–9), the discharge current grows quickly and falls slowly. In the opposite case of the small capacitance (see curve 5 in Figs. 7–9), the current grows somewhat slower than it falls.

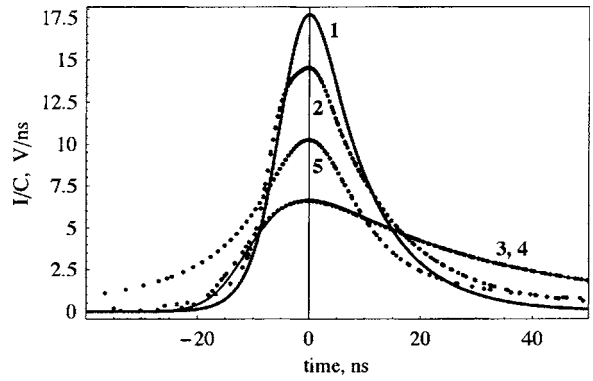

FIG. 8. The same as in Fig. 7 but for $L_g=800$ μm and $V_{\text{appl}}=450$ V.

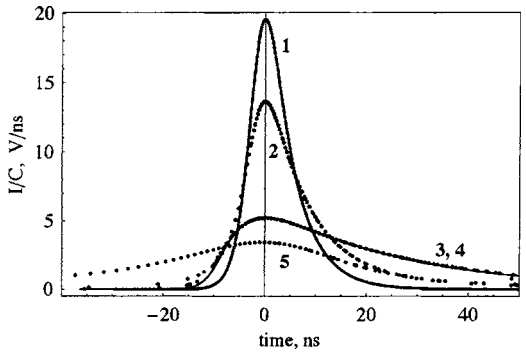

FIG. 9. The same as in Fig. 7 but for $L_g=400$ μm and $V_{\text{appl}}=320$ V.

The presented model can be extended to include, in a first approximation, plasma losses due to ambipolar diffusion to the walls surrounding the discharge volume and due to recombination by subtracting from the right-hand side of Eq. (8) the terms $\tau_{\text{dif}}^{-1}n_{\text{pc}}$ (τ_{dif} is the characteristic ambipolar diffusion time) and $k_r n_{\text{pc}}^2$ (k_r is the recombination coefficient).

V. CONCLUSION

During the development of long-gap discharges, there forms a region between the anode and cathode falls similar to a dc positive column, where the plasma density and electric field are uniform but, in contrast to a dc case, change in time. It is shown that the mechanism of the positive column uniformization has an entirely dynamic nature: it is caused by the ionization processes and has nothing to do with the diffusion of the charged particles.

A simple analytical model of long-gap discharges allowed us to obtain useful estimates for the plasma density, number of excitations and ionizations, and power consumption; it also helped to capture nontrivial trends in the dependence of the discharge current on discharge parameters.

ACKNOWLEDGMENT

The authors would like to acknowledge the Ohio Supercomputer Center for their support through Grant No. PJS0221.

APPENDIX

The quasineutrality of the plasma during the large-current stage results from the fact that Maxwellian relaxation time τ_m is much less than the time of plasma growth in the column (which is of the order of the duration of the current pulse τ_{cur}). Using the formula for plasma conductivity $\sigma\approx e\mu_e n$ and Eq. (30), one can estimate

$$\tau_m=\frac{\epsilon_0}{\sigma}\approx\frac{\epsilon_0}{e\mu_e n}\sim\frac{\epsilon_0 S}{CL_g\bar{r}(0,E_0)}=\frac{2d}{\epsilon L_g\bar{r}(0,E_0)}.$$

Since $\bar{r}(0,E_0)=\bar{r}(0,E_*)+\bar{r}(E_*,E_0)>\bar{r}(E_*,E_0)$ and, according to Eqs. (25) and (27), $\bar{r}(E_*,E_0)=r(E_*)\sim\tau_{\text{cur}}^{-1}$, the quasineutrality condition takes the form

$$\frac{\tau_m}{\tau_{\text{cur}}}\sim\frac{2d}{\epsilon L_g}\ll 1.$$

Due to this inequality, the displacement current in the positive column, $\epsilon_0 S \partial E/\partial t \sim \epsilon_0 SE/\tau_{\mathrm{cur}}$, is negligibly small compared to the electron current, $en_e\mu_e SE \sim \epsilon_0 SE/\tau_m$.

[1]J. P. Boeuf, J. Phys. D **36**, R53 (2003).
[2]O. Sahni, C. Lanza, and W. E. Howard, J. Appl. Phys. **49**, 2365 (1978).
[3]R. Veerasingam, R. B. Campbell, and R. T. McGrath, IEEE Trans. Plasma Sci. **23**, 688 (1995).
[4]R. Veerasingam, R. B. Campbell, and R. T. McGrath, IEEE Trans. Plasma Sci. **24**, 1399 (1996).
[5]J. Meunier, P. Belenguer, and J. P. Boeuf, J. Appl. Phys. **78**, 731 (1995).
[6]V. N. Khudik, V. P. Nagorny, and A. Shvydky, J. Appl. Phys. **94**, 6291 (2003).
[7]L. Weber, U.S. Patent No. 6184848B1 (2001).
[8]Yu. P. Raizer, *Gas Discharge Physics* (Springer-Verlag, Berlin, 1991).
[9]C. Punset, J. P. Boeuf, and L. C. Pitchford, J. Appl. Phys. **83**, 1884 (1998).
[10]A. Shvydky, V. N. Khudik, V. P. Nagorny, and C. E. Theodosiou, Bull. Am. Phys. Soc. **49**, 24 (2004).